

Unbalanced CRLH behavior of ferrite-loaded waveguide operated below cutoff frequency

Morteza Mohammadi Shirkolaei & Javad Ghalibafan

To cite this article: Morteza Mohammadi Shirkolaei & Javad Ghalibafan (2020): Unbalanced CRLH behavior of ferrite-loaded waveguide operated below cutoff frequency, Waves in Random and Complex Media, DOI: [10.1080/17455030.2020.1800133](https://doi.org/10.1080/17455030.2020.1800133)

To link to this article: <https://doi.org/10.1080/17455030.2020.1800133>



Published online: 03 Aug 2020.



Submit your article to this journal [↗](#)



Article views: 12



View related articles [↗](#)



View Crossmark data [↗](#)



Unbalanced CRLH behavior of ferrite-loaded waveguide operated below cutoff frequency

Morteza Mohammadi Shirkolaei ^a and Javad Ghalibafan ^b

^aDepartment of Electrical Engineering, Shahid Sattari Aeronautical University of Science and Technology, Tehran, Iran; ^bFaculty of Electrical Engineering and Robotic, Shahrood University of Technology, Shahrood, Iran

ABSTRACT

This paper proposes a new unbalance composite right/left handed (CRLH) transmission line that consists of a normally magnetized ferrite-loaded rectangular waveguide. The left-handed (LH) behavior of this structure is based on the negative effective permeability of the ferrite material and the negative effective permittivity of the hollow metallic waveguide at the frequencies below the cutoff. By increasing the frequency and passing through the cutoff frequency, this structure behaves as a right handed (RH) transmission line. As a main advantage of the proposed structure, the CRLH response of this transmission line can be tuned by changing the magnetic bias of the ferrite layer. This tunable CRLH transmission line can be used to design a tunable microwave filter or a tunable leaky wave antenna (LWA) with backfire-to-endfire scanning capability. Compare to previous CRLH metamaterial structures, the proposed structure has an easy design and a wide frequency range of tunability.

ARTICLE HISTORY


Received 24 March 2020
Accepted 20 July 2020

KEYWORDS

Composite right/left handed (CRLH); ferrite loaded-waveguide; metamaterial; negative effective permeability

1. Introduction

The composite right/left handed (CRLH) transmission lines with negative permeability and permittivity have attracted much attention because of their applications in electromagnetic absorption [1,2], leaky wave antenna (LWA) [3,4], microwave filters [5,6], and phase shifters [7,8]. The CRLH transmission lines often consist of periodic structure of metal-insulator-metal (MIM), shorted stub, split ring resonator (SRR), or complementary split ring resonator (CSRR) due to provide the negative permeability and permittivity to achieve a left-handed (LH) response [9–11]. Since the SRRs and CSRRs have a resonant behavior, most of CRLH transmission lines have a narrow frequency band of operation. To overcome this drawback, in some previous works the tunable CRLH transmission lines have been proposed, where the micro electro-mechanical switches (MEMS) [12], or pin diode, and varactor [13] have been used. The use of these elements for tuning requires electrical bias, in which the bias circuit itself distort radiation pattern for antenna applications.

CONTACT Morteza Mohammadi Shirkolaei  m.mohammadi@ssau.ac.ir; mor_mohammadi@elec.iust.ac.ir

Ferrite material is an anisotropic medium with the magnetic bias that has escaped widespread attention in both physics and engineering [14–19]. The inherent negative effective permeability of ferrite at microwave frequencies and its dependence on the magnetic DC bias, make ferrite material a good option to design of tunable CRLH transmission lines [20–25]. However, to achieve the LH response, the simultaneous negative permittivity is also needed. In this paper, a metallic hollow rectangular waveguide that operated below the cutoff frequency of dominant mode provides the negative permeability. Therefore, the ferrite-loaded waveguide operated below the cutoff frequency, as the proposed structure in this paper, can be used to achieve the CRLH response. Compared to other previous works, the proposed structure has some advantages such as wideband, high range of tunability, non-periodic and homogeneous.

The paper is organized as follows: In section 2, the effective permeability of the ferrite-filled rectangular waveguide is calculated and its tunability with the DC magnetic bias is investigated. Section 3 shows the unbalanced CRLH response of the ferrite-filled rectangular waveguide. This structure has an LH property in the frequency range wider than the previous works. However, the ferrite-filled rectangular waveguide structure has a high loss in the frequency range where the effective permeability is negative. To overcome this drawback, the ferrite-blade loaded rectangular waveguide is presented in section 4. In this section, based on the modal analysis, the dispersion diagram is calculated and validated by the numerical results. Furthermore, the tunable unbalance CRLH property of the proposed structure is investigated. Finally, in section 5 a conclusion is given.

2. Calculation of effective permeability of the ferrite-filled waveguide

The main idea in the proposed structure is combination of the negative permeability of normally magnetized ferrite and the negative effective permittivity of rectangular waveguide operated below cutoff frequency. As the first step, the effective permeability of the ferrite-filled waveguide is considered in this section. Figure 1 shows the ferrite-filled waveguide where a bias magnetic field of H_0 is applied perpendicularly to the guide plane. The permeability tensor of the z-direction biased ferrite is given by [3,26]:

$$\bar{\bar{\mu}} = \begin{bmatrix} \mu & j\mu_a & 0 \\ -j\mu_a & \mu & 0 \\ 0 & 0 & 1 \end{bmatrix} \quad (1)$$

where

$$\mu = 1 + \frac{\omega_H \omega_M}{\omega_H^2 - \omega^2}, \quad \mu_a = \frac{\omega_M \omega}{\omega_H^2 - \omega^2}, \quad \omega_H = \gamma H_0, \quad \omega_M = \gamma M_s \quad (2)$$

In these relations, M_s is the saturation magnetization, $\gamma = 2.8 \text{ MHz/Oe}$ is the gyromagnetic ratio, and ω is the operating frequency.

The relative permittivity of the ferrite material is ϵ_f . By assumption of $h \ll a$, the incident electromagnetic fields have no variation along the z-direction ($\partial/\partial z = 0$). So, the TE_{10} is the dominant mode and Maxwell's curl equations in the ferrite-filled waveguide in Figure 1 can be represented as follows:

$$\frac{\partial E_z}{\partial y} = -j\omega\mu_0\mu H_x + \omega\mu_0\mu_a H_y \quad (3)$$

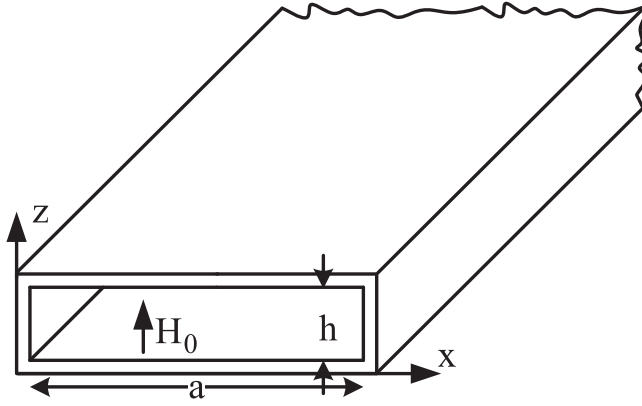


Figure 1. Ferrite-filled rectangular waveguide magnetized perpendicular to the propagation.

$$\frac{\partial E_z}{\partial x} = \omega\mu_0\mu_a H_x + j\omega\mu_0\mu H_y \quad (4)$$

$$-\frac{\partial H_x}{\partial y} + \frac{\partial H_y}{\partial x} = j\omega\varepsilon_0\varepsilon_f E_z \quad (5)$$

The transverse component of the magnetic fields can be obtained by [25]:

$$H_x = \frac{1}{\omega\mu_0(\mu_a^2 - \mu^2)} \left(\mu_a \frac{\partial E_z}{\partial x} - j\mu \frac{\partial E_z}{\partial y} \right) \quad (6)$$

$$H_y = \frac{1}{\omega\mu_0(\mu_a^2 - \mu^2)} \left(\mu_a \frac{\partial E_z}{\partial y} + j\mu \frac{\partial E_z}{\partial x} \right) \quad (7)$$

By substituting (6) and (7) into (5), the partial differential equation governs the propagation of the transverse electric field of E_z in the ferrite-filled waveguide of the Figure 1 as follows:

$$\frac{\partial^2 E_z}{\partial x^2} + \frac{\partial^2 E_z}{\partial y^2} + \omega^2 \varepsilon_0 \mu_0 \varepsilon_f \mu_{eff} E_z = 0 \quad (8)$$

where μ_{eff} is the effective permeability of the ferrite:

$$\mu_{eff} = \frac{\mu^2 - \mu_a^2}{\mu} \quad (9)$$

According to (9) and (2), the effective permeability (μ_{eff}) is varied by the frequency (ω) and the magnetic bias field (H_0) (See Figure 2).

3. LH behavior of ferrite-loaded waveguide operated below cutoff frequency

As shown in the previous section, the magnetized ferrite-loaded waveguide can be operated as a negative permeability medium. In this section, an LH behavior is achieved by a combination of negative permeability of ferrite material and plasmonic behavior of empty

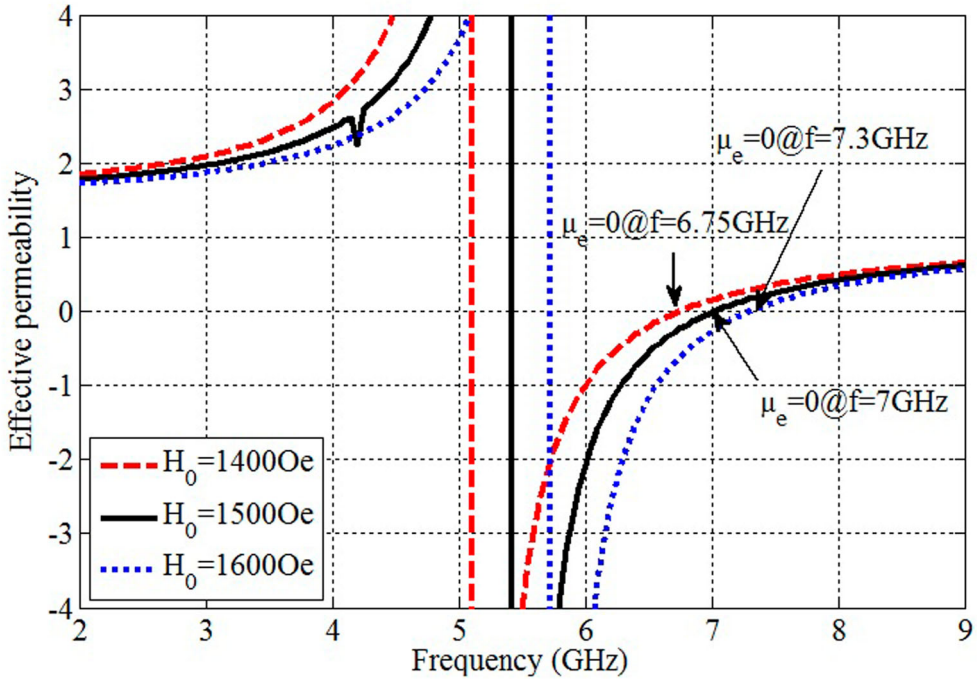


Figure 2. Effective permeability of the ferrite with $\epsilon_f = 13.2$ and $4\pi M_s = 0101T$ for different bias fields.

metal waveguide operated below the cutoff frequency. Base on the dispersion relation of this structure, the LH response is located at a frequency range where both permeability and permittivity are negative.

Synthetic plasma is the most common means of achieving a negative-passage environment, and many researchers have used one-dimensional synthetic plasma formed by a hollow metal waveguide excised below the cutoff frequency [27]. The dispersion relation for the TE_{10} mode at the waveguide in the longitudinal direction is as follows [28]:

$$\beta_{10} = \sqrt{\omega^2 \epsilon_0 \epsilon_{eff} \mu_0 \mu_{eff} - \left(\frac{\pi}{a}\right)^2} \quad (10)$$

where ω is the angular frequency, ϵ_0 is the free-pass electrical permittivity, ϵ_{eff} is the effective permittivity, μ_0 is the permeability of free space, μ_{eff} is the ferrite effective permeability, and a is the width of the wavelength. The effective permittivity, ϵ_{eff} , is obtained by the dielectric function for the no-loss plasma provided by the Drude model. This parameter is easily extracted from the properties of a rectangular waveguide below the cutoff frequency as follow [29]:

$$\epsilon_{eff} = \epsilon_f \left(1 - \frac{\omega_c^2}{\omega^2}\right) \quad (11)$$

where ϵ_f is the relative permittivity of the material inside the waveguide, and ω_c is the cutoff frequency of the waveguide [28]. For the frequencies below cutoff, due to the negative ϵ_{eff} , only evanescent mode exists in this hollow metal waveguide.

A negative permittivity is not enough for material with LH properties. Negative permeability must also be applied to achieve this feature. This property has previously been

accomplished by waveguide loading with an SRR structure with negative narrow band permeability [30]. However, ferrites have a negative effective permeability over a wider frequency range, as shown in previous section. When ferrite is biased perpendicular to the propagation of the electromagnetic wave, its effective permeability (μ_{eff}) is negative at the specified frequency range (See Figure 2). According to (9) and (2), when the DC bias is equal to zero ($H_0 = 0$), μ_{eff} is summarized as follows:

$$\mu_{\text{eff}} = \left[1 - \left(\frac{\gamma M_s}{\omega} \right)^2 \right] \quad (12)$$

In the above relation, the effective permeability is negative for $(\gamma M_s)/\omega$ greater than one. By loading a hollow rectangular metal waveguide with ferrite, an LH wave is excited in the frequency range below the cutoff (where both μ_{eff} and ϵ_{eff} are negative). In addition, the ferrite permeability can also be exploited by changes in the magnetic bias applied to the tunable and broadband LH materials.

The refractive index of the ferrite filled waveguide is obtained using the following equation:

$$n = \pm \sqrt{\mu_{\text{eff}} \epsilon_{\text{eff}}} \quad (13)$$

The positive and negative sign in (13) is used for RH and LH regions, respectively. The effective permeability (9), the effective permittivity (11), and the refractive index (13) of the ferrite-loaded waveguide are shown in Figure 3, where the magnetic bias $H_0 = 1500$ Oe, the waveguide width $a = 8$ mm, the magnetization $4\pi M_s = 0.101$ T and the relative permittivity of ferrite layer $\epsilon_f = 13.2$ (Note: the ferrite used in this structure is produced by the Japanese company muRata [21]). As shown in Figure 3, this structure has an LH property for the frequency below 6.9 GHz where both μ_{eff} and ϵ_{eff} are negative. There is a stop band in the frequency range of 6.9–7.9 GHz, where an evanescent mode is excited due to positive μ_{eff} and negative ϵ_{eff} (waveguide below the cutoff frequency). Above the frequency of 7.9 GHz, the waveguide behaves in a typical manner in the RH region. In this region, the both of μ_{eff} and ϵ_{eff} are positive. Based on Figure 3, the ferrite-filled rectangular waveguide operated below cutoff frequency behaves as an unbalanced CRLH transmission line, where there is a non-propagation frequency band between RH and LH regions.

To validate this unbalance CRLH response of the ferrite-filled rectangular waveguide, the structure of Figure 1 is simulated using HFSS software based on the finite element method (FEM). The dispersion diagram of the ferrite-filled waveguide with the specifications: $4\pi M_s = 0.101$ T and $H_0 = 1500$ Oe and $a = 8$ mm, $h = 2.1$ mm is plotted in Figure 4. The characteristic of the unbalance CRLH material is clearly illustrated in this figure. Thus, the phase velocity and the group velocity are both positive, indicating that this waveguide has an RH property at a frequency above 8 GHz. In the stop band (frequency range 6.8–7.96 GHz), phase constant is imaginary and no wave propagates. In the 5.5–6.8 GHz frequency band, when both effective permeability and effective permittivity are negative, the phase velocity is negative but group velocity is positive, confirming the existence of a backward wave as an LH medium. By comparing Figures 3 and 4, the LH, stop band and RH regions are nearly identical.

Figure 5 shows the normalized attention constant of the ferrite-filled waveguide. As shown in this figure, the insertion loss is very high in the LH region. To solve this problem in the next section, the ferrite-blade waveguide is proposed.

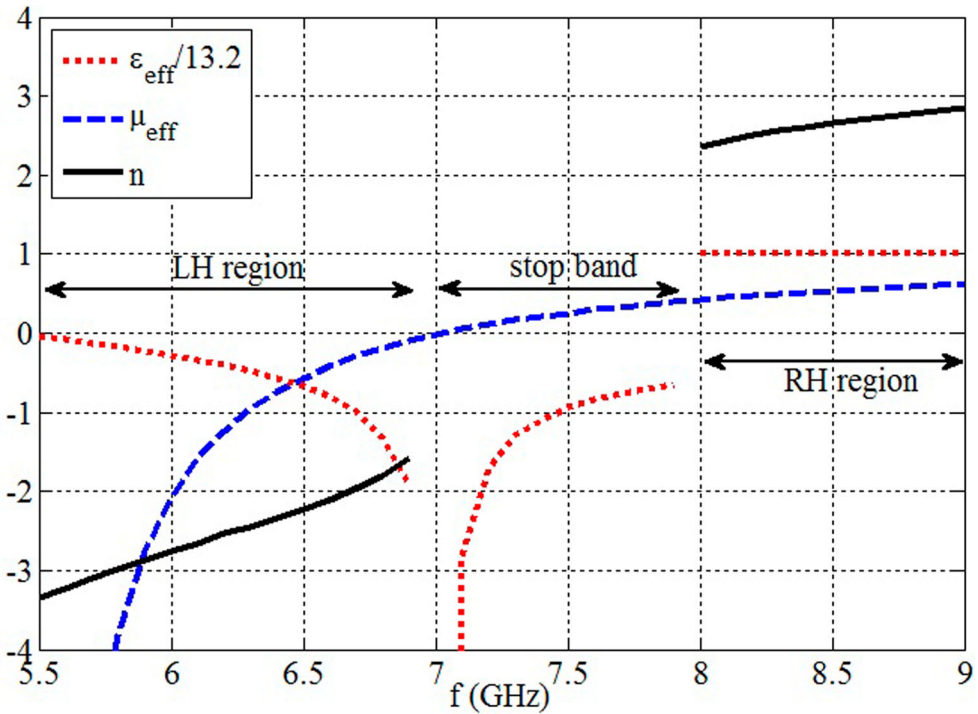


Figure 3. Effective permittivity, effective permeability, and refractive index of ferrite-filled waveguide with $H_0 = 1500$ Oe bias based on theoretical results.

4. Ferrite-blade waveguide with CRLH property

As shown in the previous section, the fully filled ferrite rectangular waveguide has high losses in the frequency range where its effective permeability is negative. So, the ferrite-filled waveguide presented in the previous section may not be a good option for designing the antenna and microwave devices. To overcome this drawback, in this section, the ferrite-blade loaded rectangular waveguide is introduced and analyzed (See Figure 6). In addition, the CRLH property of this structure and the effect of magnetic bias changes on its dispersion diagram are considered.

4.1. Modal analysis of ferrite-blade waveguide

Figure 6 shows the schematic of the proposed transversely magnetized ferrite-blade waveguide structure, where the high permittivity dielectric host ($\epsilon_d = 9.2$) fills the other space of waveguide. Based on the waveguide modal analysis, the CRLH behavior of this structure is investigated.

With assumption of the low height waveguide relative to its width, Maxwell's equations are simplified, where $(\partial/\partial z = 0)$. According to the equations presented in [25], the wave equation inside the ferrite blade is summarized as follows:

$$\left(\frac{\partial^2}{\partial x^2} + k_x^2 \right) E_z = 0 \quad \text{at} \quad g < x < g + d \quad (14)$$

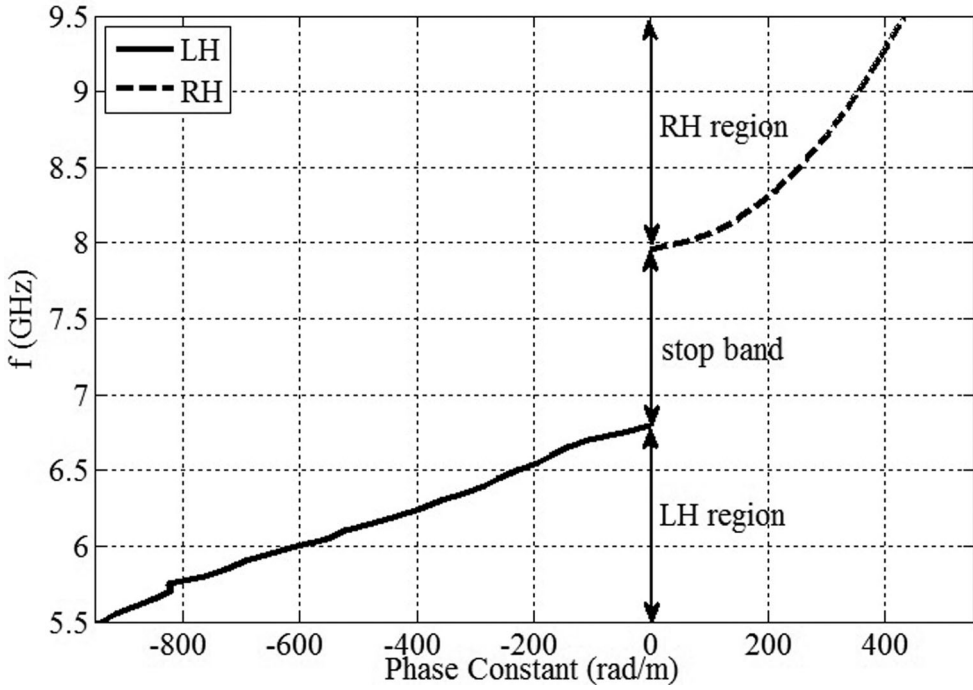


Figure 4. Ferrite waveguide dispersion graph with $a = 8$ mm and $H_0 = 1500$ Oe bias based on numerical results.

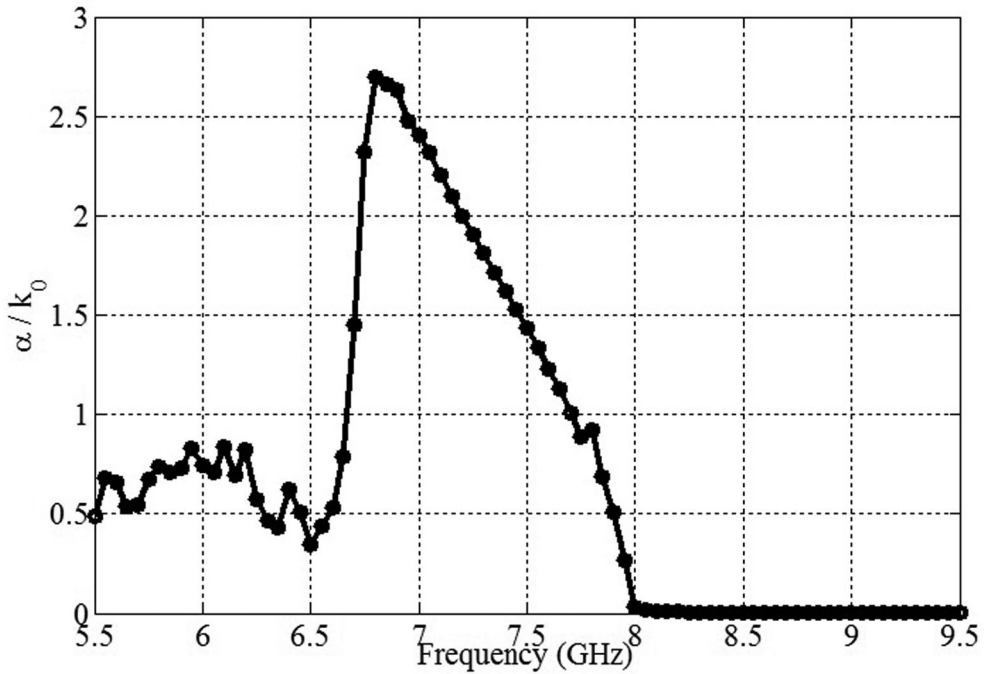


Figure 5. The normalized attenuation constant (α/k_0) of the ferrite-filled waveguide for $H_0 = 15000$ Oe.

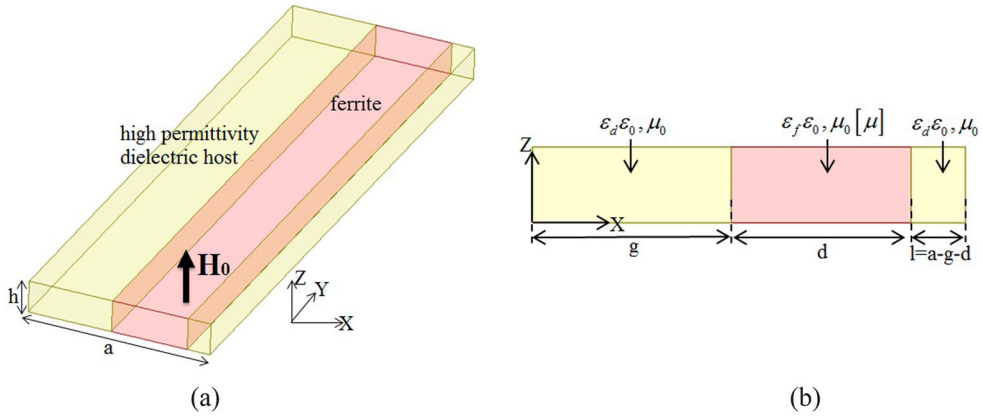


Figure 6. Ferrite-blade waveguides (a) 3D (b) Cross section view.

where

$$k_x^2 = \omega^2 \varepsilon_0 \mu_0 \varepsilon_{eff} \mu_{eff} - \beta^2 \quad (15)$$

Outside the ferrite blade, inside the dielectric, the equations are written as follows:

$$\left(\frac{\partial^2}{\partial x^2} + k_{xd}^2 \right) E_z = 0 \quad \text{at} \quad \begin{array}{l} 0 < x < g \\ g + d < x < a \end{array} \quad (16)$$

where

$$k_{xd}^2 = \omega^2 \varepsilon_0 \mu_0 \frac{\varepsilon_d}{\varepsilon_f} \varepsilon_{eff} - \beta^2 \quad (17)$$

By solving Equations (14) and (16) in general and applying boundary conditions at $x = 0$ and $x = a$:

$$E_z = A \sin(k_{xd}x) \quad \text{at} \quad 0 < x < g \quad (18)$$

$$E_z = B \sin[k_x(x - g)] + C \cos[k_x(x - g)] \quad \text{at} \quad g < x < g + d \quad (19)$$

$$E_z = D \sin[k_{xd}(a - x)] \quad \text{at} \quad g + d < x < a \quad (20)$$

By applying the four boundary conditions for the continuity E_z and H_y at $x = g$ and $x = g + d$, a collection of equations for the coefficients A , B , C , and D are obtained. By matching the electric field we have two boundaries:

$$\sin(k_{xd}g)A = C \quad (21)$$

$$\sin(k_x d)B + \cos(k_x d)C = \sin(k_{xd}l)D \quad (22)$$

where $l = a - g - d$.

The tangential magnetic field at the boundary of the two environments inside the dielectric and ferrite is calculated from the following equations:

$$H_y = \frac{1}{j\omega\mu_0} \frac{dE_z}{dx} \quad \text{at} \quad \begin{array}{l} 0 < x < g \\ g + d < x < a \end{array} \quad (23)$$

$$\begin{aligned} H_y &= \frac{1}{j\omega\mu_0(\mu^2 - \mu_a^2)} \left(\mu \frac{dE_z}{dx} - \mu_a \beta E_z \right) \\ &= \frac{1}{j\omega\mu_0\mu_{\text{eff}}} \left(\frac{dE_z}{dx} - \zeta E_z \right) \quad \text{at} \quad g < x < g + d \end{aligned} \quad (24)$$

where:

$$\zeta = \frac{\mu_a \beta}{\mu} \quad (25)$$

By applying boundary conditions for a tangential magnetic field at the boundary of two environments:

$$\mu_{\text{eff}} k_{xd} \cos(k_{xd}g)A = k_x B - \zeta C \quad (26)$$

$$\begin{aligned} [k_x \cos(k_x d) - \zeta \sin(k_x d)]B \\ - [k_x \sin(k_x d) + \zeta \cos(k_x d)]C = -\mu_{\text{eff}} k_{xd} \cos(k_{xd}l)D \end{aligned} \quad (27)$$

Assuming the ferrite blade in the center of the waveguide (symmetric state), the Equations (21), (22), (26), and (27) are in a system of four equations in four unknowns as follows:

$$\begin{cases} \sin(k_{xd}g)A = C \\ \sin(k_x d)B + \cos(k_x d)C = \sin(k_{xd}g)D \\ \mu_{\text{eff}} k_{xd} \cos(k_{xd}g)A = k_x B - \zeta C \\ [k_x \cos(k_x d) - \zeta \sin(k_x d)]B \\ - [k_x \sin(k_x d) + \zeta \cos(k_x d)]C = -\mu_{\text{eff}} k_{xd} \cos(k_{xd}g)D \end{cases} \quad (28)$$

By simplifying the above device and writing it in terms of coefficients B and C:

$$\begin{bmatrix} -k_x & \tau_+ \\ k_x \cot(k_x d) + \tau_- & -k_x + \tau_- \cot(k_x d) \end{bmatrix} \begin{bmatrix} B \\ C \end{bmatrix} = 0 \quad (29)$$

where

$$\tau_{\pm} = \mu_{\text{eff}} k_{xd} \cot(k_{xd}g) \pm \zeta \quad (30)$$

By placing the determinant of the coefficient matrix (29) equal to zero:

$$2k_x k_{xd} \cot(k_x d) \cot(k_{xd}g) + \mu_{\text{eff}} k_{xd}^2 \cot^2(k_{xd}g) - \frac{k_x^2 + \zeta^2}{\mu_{\text{eff}}} = 0 \quad (31)$$

As can be seen in the above equation, the propagation constant (β) has no dependence on the propagation direction due to the symmetry of the ferrite blade inside the waveguide.

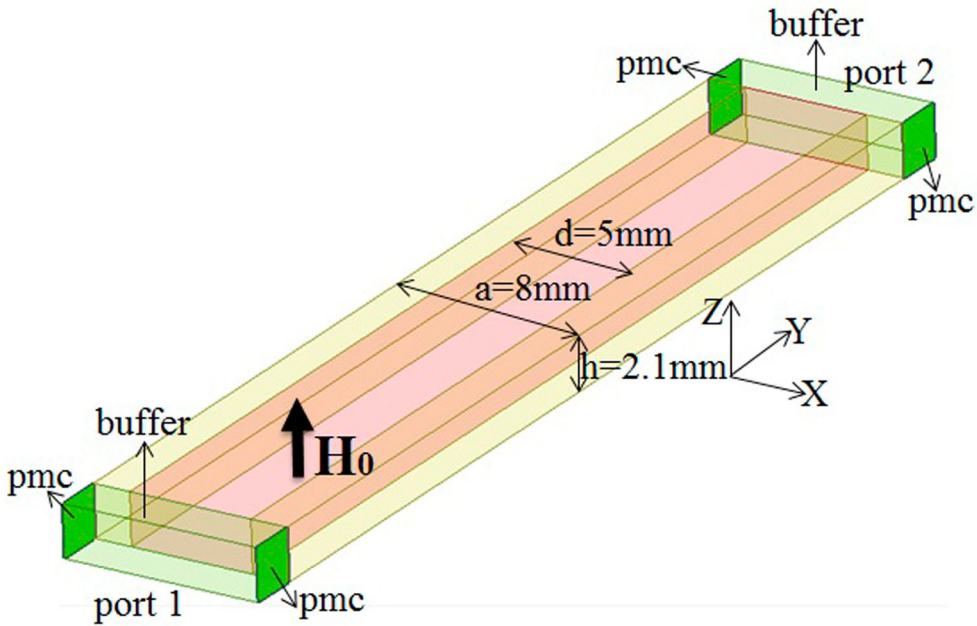


Figure 7. Schematic of the ferrite-blade waveguide in HFSS software.

The propagation constant (β) and dispersion diagram are obtained using the solution of the relation (31). There is no analytical method for solving this relation. This equation is solved using graphical and numerical methods. Newton's method is used as one of the most important methods of the rooting algorithm for solving Equation (31). Based on the above equations, the propagation constant β is a function of frequency, the effective permittivity inside the waveguide (ϵ_{eff}), the effective permeability of the ferrite (μ_{eff}), and the magnetic bias H_0 .

4.2. The CRLH and tunable response of the proposed ferrite-blade waveguide

To simplify the analysis and to prevent the production of complex waves, we consider the ferrite blade at the center of the waveguide, as shown in Figure 7. The physical parameters in this figure are $\epsilon_d = 9.2$, $a = 8$ mm, $h = 2.1$ mm, and $d = 5$ mm. In addition, the ferrite used in this structure has the characteristics of $\epsilon_f = 13.2$ and $4\pi M_s = 0101$ T. Since HFSS port models cannot be directly connected to an anisotropic environment, two buffers with waveguide structures at the two ends of the structure are used where the relative permittivity of the buffers is $\epsilon_d = 9.2$. Due to the small width of the waveguide and its working below the cutoff frequency, the narrow wall of the buffers is considered as the perfect magnetic conductor (PMC). Figure 8 compares the analytical dispersion relation given in (31) and the simulated one based on the finite element method (FEM) at HFSS software. The dispersion diagram obtained by the simulation only relates to the blade-ferrite waveguide because the effect of the buffer phases is neglected. As shown in Figure 8, the simulated results validate the analytical results of modal analysis in the previous section. The results show that

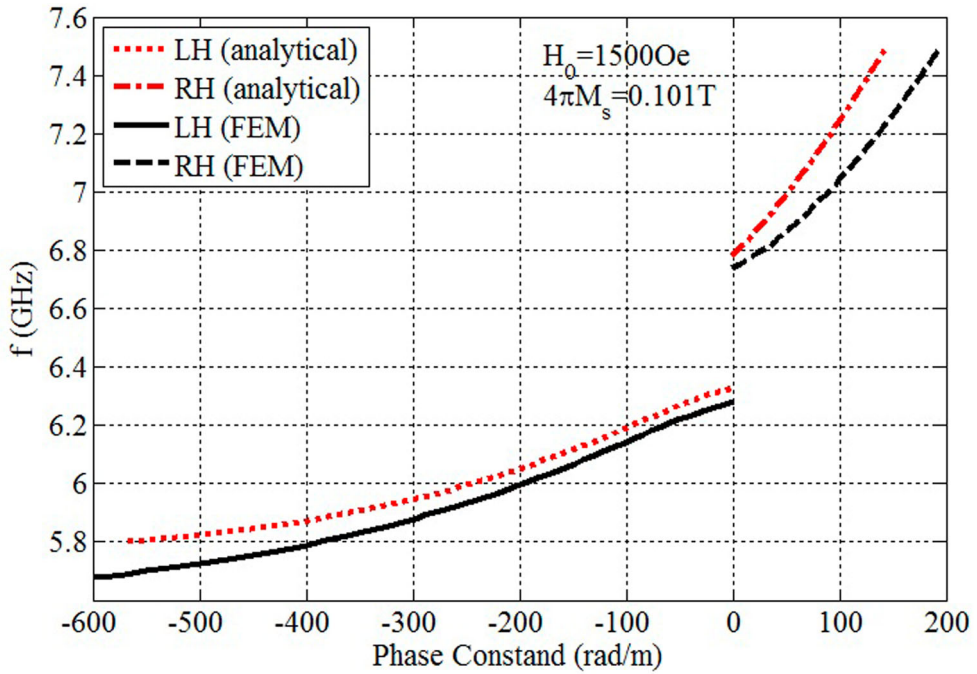


Figure 8. Dispersion diagram of the ferrite-blade waveguide at its center obtained by the analytical method and full-wave simulation.

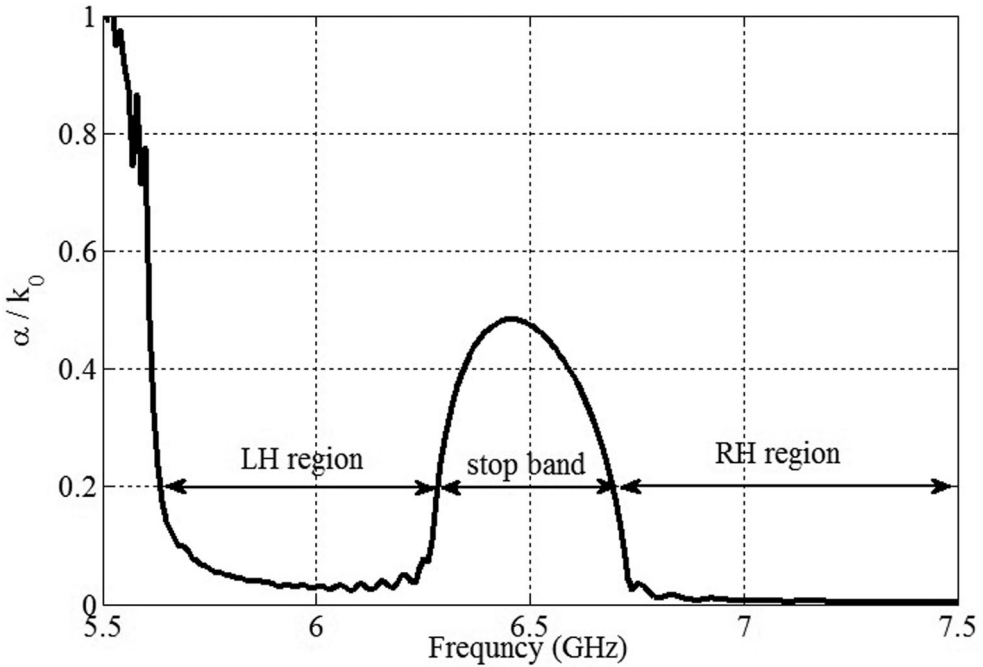


Figure 9. The normalized attenuation constant (α/k_0) of the ferrite-blade waveguide for $H_0 = 1500 \text{ Oe}$.

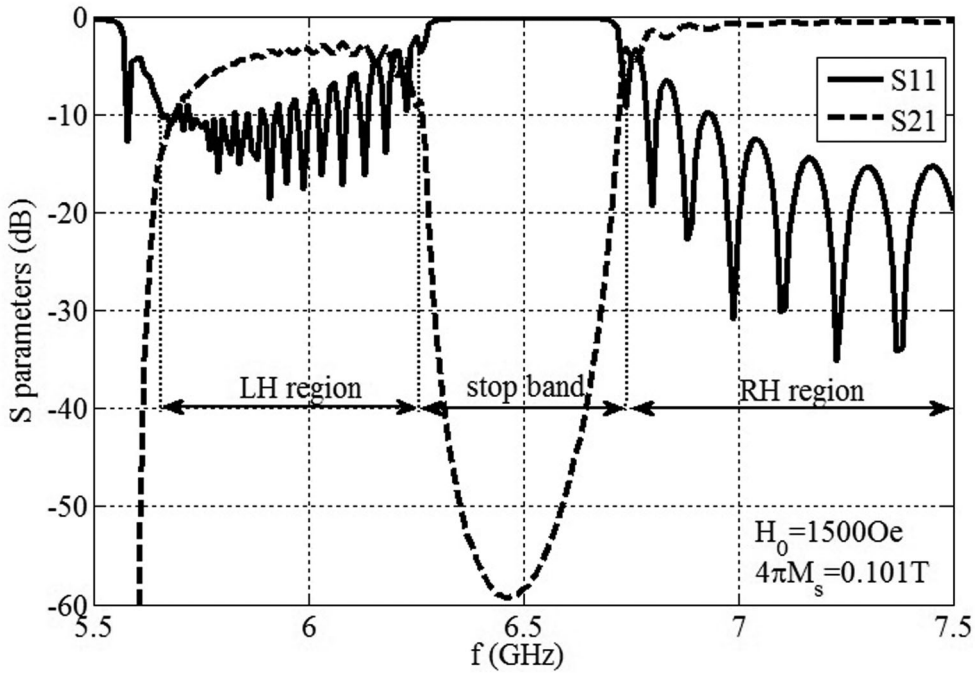


Figure 10. Scattering parameters of the ferrite-blade waveguide with $H_0 = 1500\text{Oe}$.

the proposed structure has an unbalanced CRLH response, where a non-propagation band gap is located between the LH and RH regions.

By comparing Figures 4 and 8, we conclude that bandgap of the ferrite-filled waveguide (6.8–7.9 GHz) is wider than the ferrite-blade waveguide (6.3–6.8 GHz). As an advantage, since the ferrite blade does not include the whole waveguide, its insertion loss (S_{21}) in the LH range is less than the ferrite-filled waveguide. Figure 9 confirms that the insertion loss of this structure in the LH region is low (compare with Figure 5). This feature is suitable for antenna design to achieve high efficiency. Figure 10 shows the scattering parameters of the ferrite-blade waveguide with the dimensions given in Figure 7.

To evaluate the CRLH behavior of the ferrite-blade waveguide, the electric field distribution of this structure is shown in Figure 11 at two different frequencies of 6 and 7.2 GHz in LH and RH band, respectively. As shown in Figure 11 (a), the phase velocity and group velocity are in opposite directions, confirming the LH response at low frequencies. At higher frequencies in the RH region, the phase velocity and group velocity are the same direction (Figure 11(b)). This confirms that the ferrite-blade waveguide has a CRLH response.

The dispersion diagram of the ferrite-blade waveguide under the bias of $H_0 = 1400, 1500, 1600\text{Oe}$ is shown in Figure 12. As shown in the figure, the proposed structure has a tunable CRLH response. The frequency of the LH and RH regions shifts upward as the magnetic bias increases. Due to the tunable CRLH feature, this structure can be used for the design of tunable band-stop filters and tunable continuous backward-to-forward beam-scanning antennas.

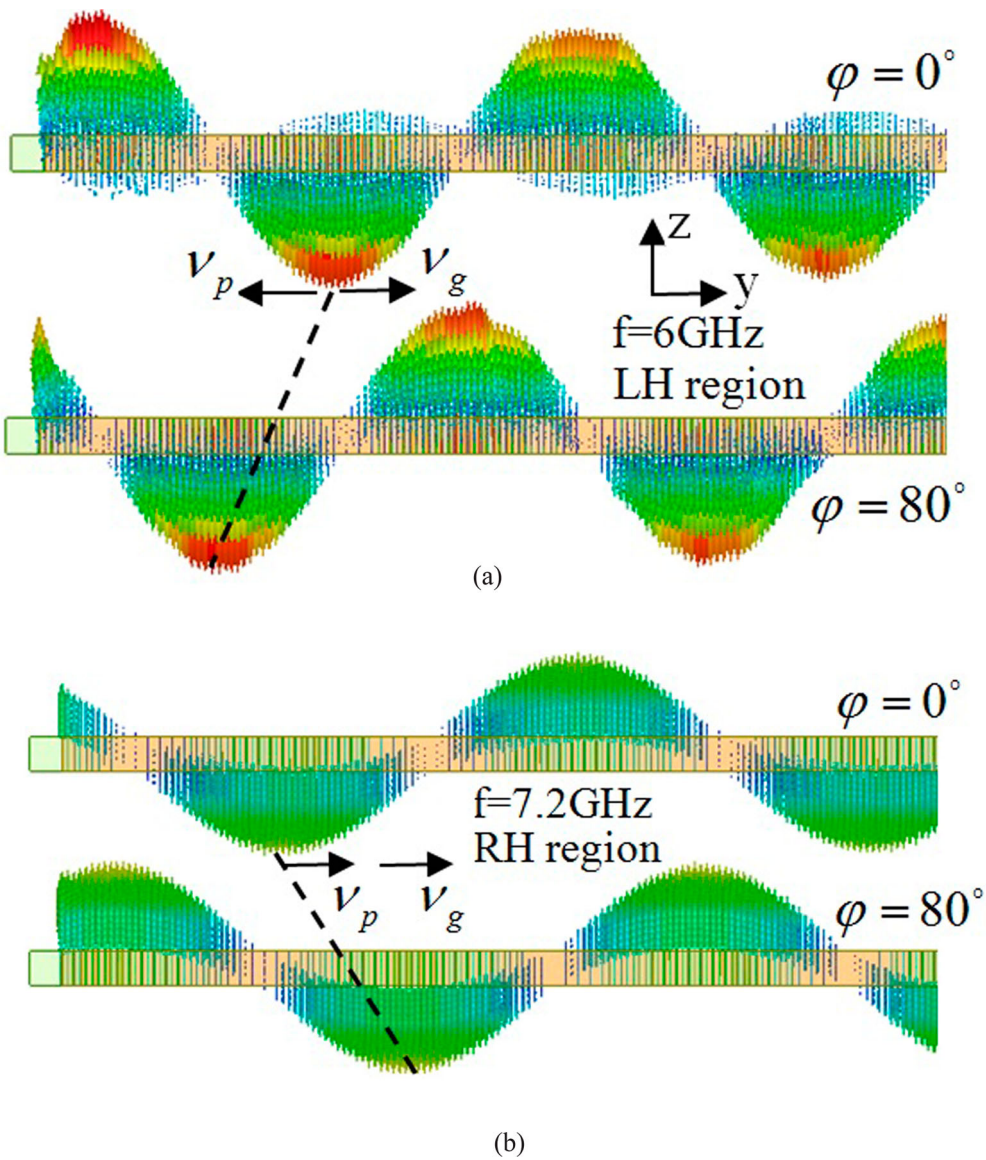


Figure 11. Electric field distribution along the structure with $H_0 = 1500$ Oe (a) LH region (b) RH region.

5. Conclusion

A new unbalance CRLH transmission line that consists of a magnetized ferrite-loaded rectangular waveguide is proposed. In fact, in the proposed structures, the inherent negative of normally magnetized ferrite layer is combined with the negative permittivity of rectangular waveguide operated below the cutoff frequency. Based on simulated and analytical results, the CRLH response of the ferrite-loaded rectangular waveguide can be tuned by the magnetic DC bias. Compare to the ferrite-filled waveguide, the ferrite-blade waveguide is low loss and more efficient. So, the ferrite-blade rectangular waveguide can be used to design

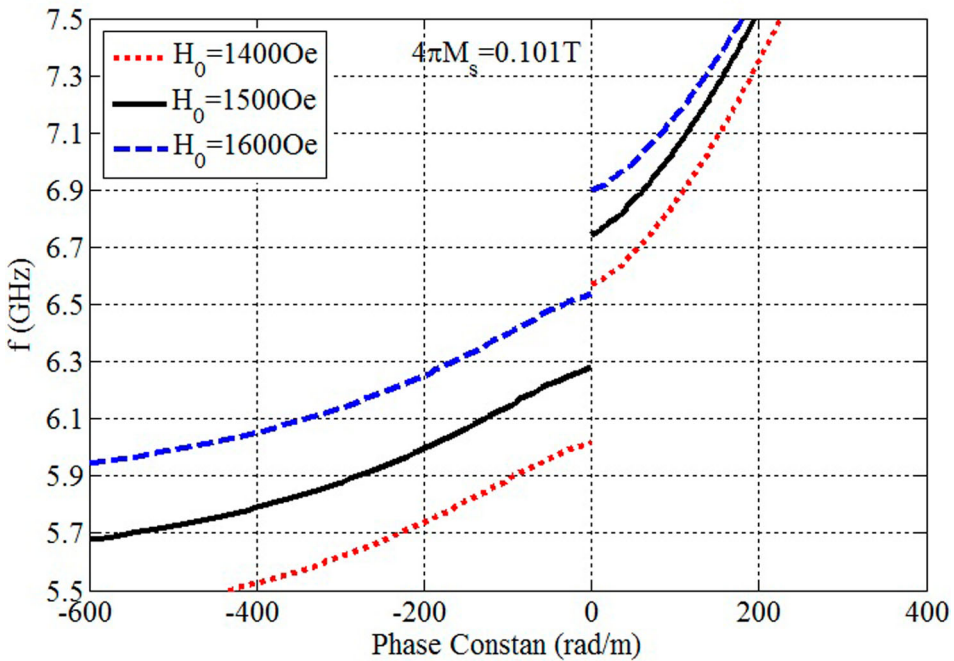


Figure 12. Dispersion diagram of the ferrite-blade waveguide under different magnetic biases with physical parameters mentioned in Figure 7.

a tunable microwave filter or a tunable leaky wave antenna (LWA) with backfire-to-endfire scanning capability.

Disclosure statement

No potential conflict of interest was reported by the author(s).

ORCID

Morteza Mohammadi Shirkolaei  <http://orcid.org/0000-0001-5442-7358>

Javad Ghalibafan  <http://orcid.org/0000-0001-7113-0951>

References

- [1] Xiao Z, Lv F, Li W, et al. A three-dimensional ultra-broadband and polarization insensitive metamaterial absorber and application for electromagnetic energy harvesting. *Waves Random Complex Media*. 2020:1–9. doi:10.1080/17455030.2020.1733705.
- [2] Zhou BC, Wang DH, Ma JJ, et al. An ultrathin and broadband radar absorber using metamaterials. *Waves Random Complex Media*. 2019:1–10. doi:10.1080/17455030.2019.1634301.
- [3] Mohammadi M, Kashani FH, Ghalibafan J. Backfire-to-endfire scanning capability of a balanced metamaterial structure based on slotted ferrite-filled waveguide. *Waves Random Complex Media*. 2019: 1–15. doi:10.1080/17455030.2019.1654148.
- [4] Kumar N, Chakraborty O, Agarwal R, et al. A CRLH leaky wave antenna on SIW with continuous scan using novel S-slots. *International Journal of Electronics Letters*. 2018;6:459–467.

- [5] Yang S, Chen Y, Yu C, et al. Super compact and ultra-wideband bandpass filter with a wide upper stopband based on a SCRLH transmission-line unit-cell and two lumped capacitors. *J Electromagn Waves Appl.* **2019**;33:350–366.
- [6] Zermane A, Sauviac B, Djouablia L, et al. Tunability of metamaterial compact band-stop filters using YIG substrate. *J Electromagn Waves Appl.* **2019**;33:1726–1734.
- [7] Zhang J, Cheung SW, Yuk TI. Design of n-bit digital phase shifter using single CRLH TL unit cell. *Electron Lett.* **2010**;46:506–508.
- [8] Choi S, Su W, Tentzeris MM, et al. A Novel Fluid-Reconfigurable Advanced and Delayed Phase Line using Inkjet-Printed Microfluidic Composite right/left-Handed Transmission Line. *IEEE Microwave Compon Lett.* **2015**;25:142–144.
- [9] Aznabet M, El Mrabet O, Marie Floc'h J, et al. A coplanar waveguide-fed printed antenna with complementary split ring resonator for wireless communication systems. *Waves Random Complex Media.* **2015**;25:43–51.
- [10] Caloz C, Itoh T. *Electromagnetic metamaterials: transmission line theory and microwave applications.* Hoboken (NJ): Wiley; **2006**.
- [11] Roy S, Chakraborty U. Metamaterial-embedded dual wideband microstrip antenna for 2.4 GHz WLAN and 8.2 GHz ITU band applications. *Waves Random Complex Media.* **2018**. doi:10.1080/17455030.2018.1494396.
- [12] Cetiner BA, Crusats GR, Jofre L, et al. RF MEMS integrated frequency reconfigurable annular slot antenna. *IEEE Trans. Antennas Propag.* **2010**;58:626–632.
- [13] Patel SK, Shah KH, Kosta YP. Frequency-reconfigurable and high-gain metamaterial microstrip-radiating structure. *Waves Random Complex Media.* **2018**. doi:10.1080/17455030.2018.1452309.
- [14] Bi K, Zhu W, Lei M, et al. Magnetically tunable wideband microwave filter using ferrite-based metamaterials. *Appl. Phys. Lett.* **2015**;106:173507.
- [15] Zhao H, Zhou J, Kang L, et al. Tunable two-dimensional left-handed material consisting of ferrite rods and metallic wires. *Opt Express.* **2009**;17:13373–13380.
- [16] Lei M, Feng N, Wang Q, et al. Magnetically tunable metamaterial perfect absorber. *J Appl Phys.* **2016**;119:244504–1. -5.
- [17] Bi K, Zhou J, Zhao H, et al. Tunable dual-band negative refractive index in ferrite-based metamaterials. *Opt Express.* **2013**;21:10746–10752.
- [18] He G, Wu R-x, Poo Y, et al. Magnetically tunable double-negative material composed of ferrite-dielectric and metallic mesh. *J Appl Phys.* **2010**;107:093522–1. -5.
- [19] He P, Gao J, Chen Y, et al. Q-band tunable negative refractive index metamaterial using Sc-doped BaM hexaferrite. *J Phys D: Appl Phys.* **2009**;42:155005.
- [20] Kumar T, Kalyanasundaram N, Lande BK. A generalized case of the electromagnetic scattering from an array of ferrite cylinders. *Waves Random Complex Media.* **2015**;25:587–607.
- [21] Kodera T, Caloz C. Uniform ferrite-loaded open waveguide structure with CRLH response and its applications to a novel back fire-to-end fire leaky wave antennas. *IEEE Trans. Microw. Theory Tech.* **2009**;75:784–795.
- [22] Kodera T, Caloz C. Integrated leaky wave antenna- duplexer/duplexer using CRLH uniform ferrite-loaded open waveguide. *IEEE Trans. Ant. and Propag.* **2010**;57:2508–2514.
- [23] Kargar E, Ghalibafan J. Tunable ferrite-based metamaterial structure and its application to a leaky-wave antenna. *J. Magn. Magn. Mater.* **2018**;456:223–227.
- [24] Hwang KC, Eom HJ. Radiation from a ferrite-filled rectangular waveguide with multiple slits. *IEEE Microw. Wire. Comp. Lett.* **2005**;15:345–347.
- [25] Mohammadi M, kashani FH, Ghalibafan J. A partially ferrite-filled rectangular waveguide with CRLH response and its application to a magnetically scannable antenna. *J. Magn. Magn. Mater.* **2019**;491; doi:10.1016/j.jmmm.2019.165551.
- [26] Ghalibafan J, Komjani N, Rejaei B. Tunable left-handed characteristics of ferrite rectangular waveguide periodically loaded with complementary split-ring resonators. *IEEE Trans. Magn.* **2013**;49:4780–4784.
- [27] Jackson JD. *Classical electrodynamics.* New York: Wiley; **1999**.
- [28] Balanis CA. *Advanced engineering electromagnetics.* 2nd ed. New York: Wiley; **2012**.

- [29] Dechant A, Okoniewski M. Broadband double negative material from ferrite-loaded metallic waveguides. *Electron Lett.* [2006](#);42:4–7.
- [30] Marques R, Martel J, Mesa F, et al. Left-handed-media simulation and transmission of EM waves in subwavelength split-ring resonator- loaded metallic waveguide. *Phys. Rev. Lett.* [2002](#);89:1–4.